

Structural studies of Mn⁺ implanted GaN film

Y. Shi†, L. Lin, C. Z. Jiang, and X. J. Fan

Accelerator Lab, Department of Physics, Wuhan University, Wuhan 430072, China

Abstract

Wurtzite GaN films are grown by low-pressure MOCVD on (0001)-plane sapphire substrates. The GaN films have a total thickness of 4 μm with a surface Mg-doped p-type layer, which has a thickness of 0.5 μm . 90keV Mn⁺ ions are implanted into the GaN films at room temperature with doses ranging from 1×10^{15} to 1×10^{16} cm^{-2} . After an annealing step at 770°C in flowing N₂, the structural characteristics of the Mn⁺ implanted GaN films are studied by X-ray diffraction (XRD), Rutherford backscattering spectrometry (RBS) and atomic force microscopy (AFM). The structural and morphological changes brought about by Mn⁺ implantation and annealing are characterized.

Keywords : GaN film; ion implantation

1. Introduction

Gallium nitride (GaN) is a wide-band-gap III-V compound semiconductor material, which can be used to produce blue-light-emitting diodes and lasers, as well as high-temperature and high-power devices. While manganese (Mn) represents a potential acceptor in GaN, Mn-doped GaN may form an interesting diluted magnetic semiconductor, which might have a Curie temperature above room temperature and thus have a great potential for the fabrication of magneto-electrical and magneto-optical devices [1-3]. But there is a major obstacle in making III-V semiconductors magnetic, i.e., the low solubility of magnetic elements (*e.g.* Mn) in these compounds [4].

It is well known that ion implantation has the advantage to introduce impurities without any limitation of solubility. Additionally, it provides the advantage to reproducibly generate high doping level. So ion implantation into GaN, followed by an annealing step, can be successfully applied for several technological steps in the fabrication of GaN-based devices [5].

The Mn⁺ implantation characteristics of GaN have been investigated [6] and it is suggested that low energy and dosage of implantation is favorable of the recovery of implant damage. As there is few report about the implantation of p-type GaN by now, 90keV Mn⁺ ions are implanted into p-type GaN films at room temperature with doses ranging from 1×10^{15} cm^{-2} to 1×10^{16} cm^{-2} . After an annealing step at 770°C in flowing N₂, the structural characteristics and morphological changes of the Mn⁺ implanted GaN films are studied.

2. Experiment

The GaN films were grown by low-pressure metal organic chemical deposition (MOCVD) on (0001)- plane sapphire substrates. An undoped GaN layer with a thickness of 3.6 μm was grown at 1030°C. Then the Mg-doped GaN, which has a thickness of 0.5 μm , was grown upon the undoped GaN at 1010°C. Electrical activation of the prepared GaN layers was achieved by annealing in nitrogen at 760°C for 30 minutes. Hall measurements showed that the hole concentration in

† E-mail : sz1028@sohu.com

the p-type GaN film was in the range of $1 \times 10^{17} - 3 \times 10^{17} \text{ cm}^{-3}$.

Mn⁺ ions with beam flux of $5 \mu\text{A}$ were implanted into the Mg-doped p-type GaN films at room temperature with an energy of 90 keV and doses ranging from 1×10^{15} to $1 \times 10^{16} \text{ cm}^{-2}$. The subsequent rapid thermal annealing (RTA) was carried out at 770°C for 45 s and 90 s under flowing N₂. During the annealing, the samples were covered by another p-type GaN sample to suppress the escape of the volatile component. The effects of Mn⁺ implantation and annealing on the structural characteristics of the GaN films were studied by X-ray diffraction (XRD), Rutherford backscattering spectrometry (RBS) and atomic force microscopy (AFM).

3. Results and Discussion

XRD spectra measured use Cu K_{α1} line are shown in Fig. 1. For all the GaN films, either implanted or

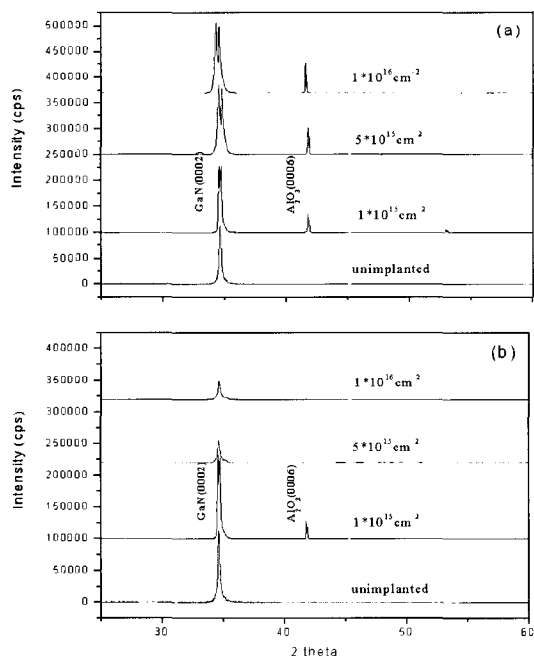


Fig. 1. XRD spectra of GaN films. Different implant doses are labeled above the curves. The implanted GaN films are annealed at 770°C for (a) 45s and (b) 90s.

unimplanted, the XRD spectra exhibit a sharp peak of wurtzite GaN(0002) at $2\theta = 34.6^\circ$, which can be used to judge the crystallinity of GaN films. The implanted samples in Fig. 1(a) have almost the same intensity of the GaN(0002) peak, but the peak width increases with the implant dose. This means the coherent length in the GaN lattice decreases with the increasing of implant dosages. Obvious changes of GaN(0002) peak intensity occur in Fig. 1(b), where the annealing of 90s at 770°C affects the crystallinity of implanted GaN films, especially for the samples implanted with relatively high dose of $1 \times 10^{16} \text{ cm}^{-2}$.

The distribution of the 90keV implanted Mn⁺ ions in GaN films is simulated with TRIM code, which shows a deviation of 150 \AA around a mean projected range of about 400 \AA . As the conventional XRD spectra show mainly the bulk information, the effects of Mn⁺ implantation in the GaN surface layer is checked by RBS technique with 1.8MeV He^+ . Figure 2 shows the RBS spectra of Mn⁺ implanted GaN films.

As it is difficult to profile light element (e.g. N, Mn) in heavy element (here Ga) matrix and the GaN film is very thick ($4 \mu\text{m}$), the measured RBS spectra disclose mainly the depth distribution of Ga concentration. The normalized RBS random spectra in Fig. 2 indicate that the concentration of Ga in the GaN surface layer changes with the implanting dosages. Part reason for this may be the substitutionality of Ga by Mn is different under different levels of implanting [6,7].

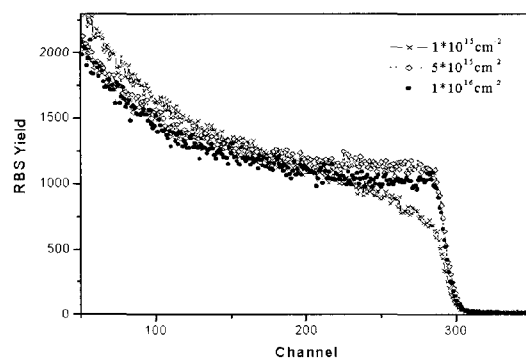


Fig. 2. RBS spectra of Mn⁺ implanted GaN films, which are annealed at 770°C for 90s.

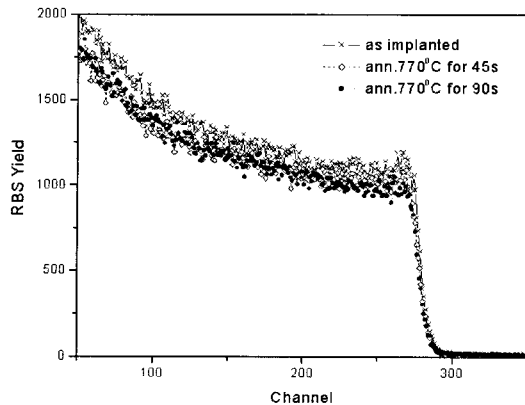


Fig. 3. RBS spectra of Mn^+ implanted GaN films with dose of $1 \times 10^{16} \text{ cm}^{-2}$.

Figure 3 shows the normalized RBS random spectra for Mn^+ implanted GaN films with dose of $1 \times 10^{16} \text{ cm}^{-2}$. A weak decrease of Ga concentration in the surface layer occurs when annealing time extends. The results show that the annealing improves the substitution of Ga in the same Mn^+ implanted GaN layer [6].

The morphological changes brought about by Mn^+ ion implantation and annealing are investigated by AFM. The AFM morphology of un-implanted GaN films is shown in Fig. 4(a), which has the main feature of wurtzite GaN hexagonal prism and crystal terrace. Figure 4(b) shows the AFM image of Mn^+ implanted GaN films with dose of $5 \times 10^{15} \text{ cm}^{-2}$, which is annealed at 770°C for 45s. In the same scanning area of $15 \times 15 \mu\text{m}$, Mn^+ implantation and annealing destruct the crystal surface and make the surface amorphous-like. Nevertheless, the surface roughness decreases from over 100 nm to less than 50 nm. The modification of the surface layer may affect the magnetic property studies of Mn^+ implanted GaN films, which are undergoing and will be reported elsewhere.

4. Conclusions

P-type GaN films are doped by 90 keV Mn^+ implantation. The crystallinity of GaN films worsens with annealing at 770°C for 90s at relatively high dosage. The substitutionality of Ga in the implant layer changes

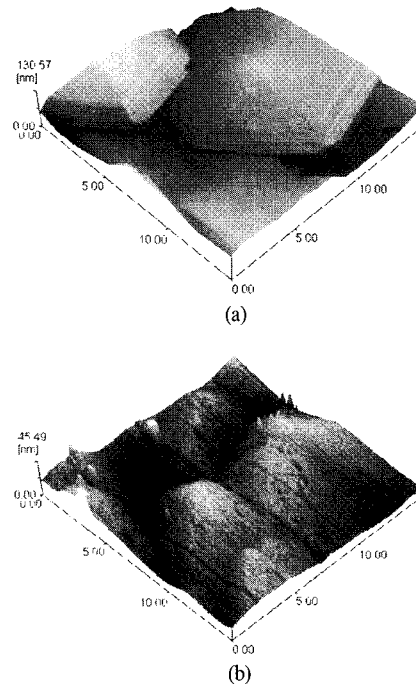


Fig. 4. AFM images of GaN. (a) un-implanted, (b) implanted with Mn^+ at $5 \times 10^{15} \text{ cm}^{-2}$.

with different dosages and annealing times. In the same time, the surface morphology of GaN is modified by the implantation and annealing. Implanting dosage and annealing play an important role in these dynamical processes.

Acknowledgments

The work is funded by the National Natural Science Foundation of China (No. 10205010) and the Laboratory of Nuclear Analysis Techniques (LNAT), Chinese Academy of Sciences. The support from the Scientific Research Foundation for ROCS, State Education Ministry, is also gratefully acknowledged.

References

- [1] T. Diel, H. Ohno, F. Matsukura, J. Cibert, and D. Ferrand, *Science* **287**, 1019 (2000).
- [2] S. Sonoda, S. Shimizu, T. Sasaki, Y. Yamamoto,

- and H. Hori, *J. Cryst. Growth* **237-239**, 1358 (2002).
- [3] J. M. Baik, H. W. Jang, J. K. Kim, and J.-L. Lee, *Appl. Phys. Lett.* **82**, 583 (2003).
- [4] H. Ohno, *Science* **281**, 951 (1998).
- [5] C. Liu, A. Wenzel, J. W. Gerlach, X. J. Fan, and B. Rauschenbach, *Surf. Coat. Tech.* **128-129**, 455 (2000).
- [6] C. Liu, E. Alves, A. R. Ramos, M. F. da Silva, J. C. Soares, T. Matsutani, and M. Kiuchi, *Nucl. Instr. and Meth. B* **191**, 544 (2002).
- [7] S. O. Kucheyev, J. S. Williams, J. Zou, C. Jagadish, and G. Li, *Nucl. Instr. and Meth. B* **178**, 209 (2001).